Proceedings in MANUFACTURING SYSTEMS

Proceedings in Manufacturing Systems, Volume 9, Issue 1, 2014, 207-214 ISSN 2067-9238

ANALYSIS OF MACHINING FORCES IN LIGHT-FORCE ROBOTIC MILLING OF ALUMINIUM PARTS

Adrian Florin NICOLESCU[1,*], Andrei Mario IVAN[2], Cezara Georgia COMAN[3]

[1)] PhD, Prof., Machines and Manufacturing Systems Department, University "Politehnica" of Bucharest, Romania
[2)] PhD, Lecturer, Machines and Manufacturing Systems Department, University "Politehnica" of Bucharest, Romania
[3)] PhD, Lecturer, Machines and Manufacturing Systems Department, University "Politehnica" of Bucharest, Romania

Abstract: *This article presents the work performed by the authors in the field of light-force robotic milling of aluminium parts. The research is focused on applications in which an articulated arm, low payload robot manipulates the milling-type deburring tool around an aluminium workpiece, which is clamped on a Kistler 9257B dynamometer which measured the machining forces. The main objective of the research was to develop an analysis of machining forces in low-power robotic milling applications through experimental data acquisition. The experimental equipment consisted of an articulated arm, 6 DOF Kawasaki FS10E industrial robot with 10 kg payload and a Kistler 9257B dynamometer capable of measuring the machining forces on three orthogonal directions corresponding to X, Y and Z axes of the part coordinate system. The robot was equipped with an ATI RC-340 radially compliant deburring tool. The experimental procedure was conducted by performing a chamfering operation on the lateral edges of an aluminium part. The robot program was developed using the point-to-point block teaching method on the teach-pendant. The program was then run several times, with gradually increased depth of cut and various feed rates. The results after each program run were observed by visual inspection and through data collected by the Kistler dynamometer. Based on these observations, the conclusions were drawn regarding the milling efficiency in each situation and the influence of machining forces on robot behaviour.*

Key words: *robotic milling, machining forces, edge chamfering, dynamometer, force measurement.*

1. INTRODUCTION

Industrial robotics has known a continuous growth in the past decades. Starting with the earliest applications of spot welding and assembly, the scope of robotics has grown to include almost every industrial area. Due to high programmability and kinematic flexibility, industrial robots have taken over many tasks previously performed by hand or through other inefficient methods. Having certain advantages, industrial robots have been integrated even in areas were other well-developed equipments were available, such as machining. However, robots were never seen in the field of machining as replacements for machine-tools, but as complementary equipment. The tasks performed by industrial robots integrated into machining applications are split into two branches: machine tending and robotic machining. Thus, while some other widely implemented robotic applications – such as painting, arc welding, spot welding, assembly, palletizing, and material handling – have gained a certain level of maturity, the growing area of robotic machining also represents today a major research direction [1, 2].

The areas where industrial robots are well equipped for performing the necessary tasks are generally linked to low-to-medium force machining operation with low depth of cuts performed on complex-shaped parts. While having the disadvantages of lower stiffness, horsepower and precision when compared to machine tools, the robots perform better in the areas of kinematic flexibility and programmability. Thus, when high precision and heavy cuts are not required, industrial robots may be a cheaper and more flexible solution, especially if the shape of the part requires complex trajectories.

Two of the most widely encountered machining operations are edge chamfering and deburring. Furthermore, these operations also often require part contour tracking and complex-shaped trajectories, while being not so demanding when it comes to machining forces. Thus, being suitable for robotic integration, the research presented in this paper was focused on analyzing the machining forces for robotic chamfering, taking into account that deburring operations were studied using another experimental procedure involving plastic parts – robotic deburring being more representative for this kind of workpiece material [1].

There are currently two main approaches in robotic milling [2, 3]: the robot can manipulate the milling tool around the workpiece, which is clamped on a fixture (as shown in Fig. 1) [4] or the milling tool can be mounted on a fixed support and the robot can manipulate the workpiece around it (as shown in Fig. 2) [5].

[*] Corresponding author: Splaiul Independentei 313,
Tel.: +40721800625;
E-mail addresses: *afnicolescu@yahoo.com* (A. Nicolescu), *andrei.mario@yahoo.com* (M. Ivan), *cezara.avram@yahoo.com* (C. Coman)

Fig. 1. Milling application with the robot manipulating the tool.

Fig. 2. Deburring application with the robot manipulating the workpiece.

The main weakness of the industrial robots with respect to machining applications is the low stiffness when compared to machine tools [6]. Thus, robots are only suitable for machining operations which require relatively low forces. Taking into account that the milling forces are mainly influenced by workpiece material, feeds and speeds and depth of cut, there can be concluded that efficient robotic milling operations can be performed mainly on soft materials.

Taking into account the above context, the scope of the research described in this paper is limited to applications in which the robot manipulates the milling-type deburring tool around an aluminium workpiece, which is clamped on a fixture. Also, the robot used for experimental determination has a very low payload of 10 kg. Because a successful robotic milling application depends on the level of the machining forces – which, especially for low payload robots, must be kept at acceptable values in order to be absorbed by the robot – the main goal of the research was to measure those forces, decomposed along the three axes of the part coordinate system.

Another goal of the research was to observe the behaviour of a radially compliant end-effector integrated in a milling application. While these tools are usually equipped for deburring application, the radial compliance is a passive force control method which has the main purpose to ensure good and constant contact between the tool and the part, a feature that can be useful for other low-force milling applications. Thus, the experimental procedure was set so that the ability of the radially compliant end-effector to follow part edge irregularities while maintaining a robust cutting behaviour could be observed. Also, another advantage of using this setup is the possibility to evaluate the capability of a radially compliant tool to perform aluminium milling operations, taking into account that, above certain values of machining forces, the tool would be deflected away from the programmed trajectory as a result of compliance effect.

Regarding force measurement, there are two possible approaches: the force sensor can be placed between the robot's wrist flange and the end-effector (as shown in Fig. 3) [7] or it can be placed between the workpiece and the workpost table (as shown in Fig. 4) [8]. The experimental setup used for this research followed the second approach – it must be taken into account that a force sensor mounted on the robot's wrist flange also affects the payload of the robot.

2. EXPERIMENTAL EQUIPMENT

The analysis of aluminium milling application was done using an experimental approach. The chamfering operations were performed by a Kawasaki FS10E articulated-arm robot with 6 degrees of freedom, including a Kawasaki D controller (shown in Fig. 5). The functional parameters of the robot are shown in Table 1 [9]. The robot was equipped with an ATI QC41 automatic tool changer and an ATI RC-340 end-effector (shown in Fig. 6) [10]. The functional parameters of the end-effector are shown in Table 2 [10].

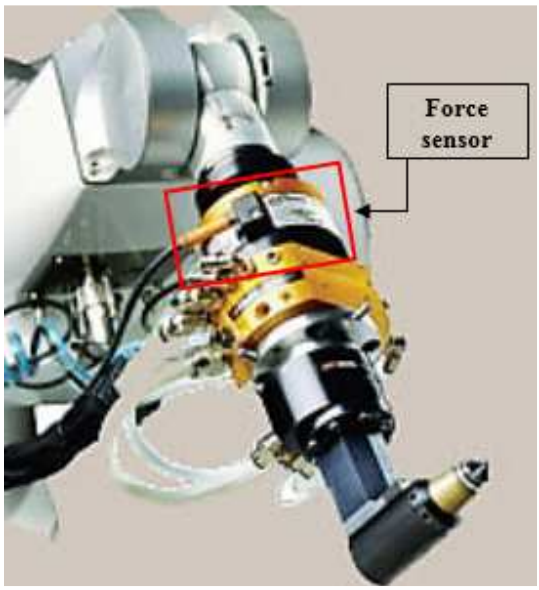

Fig. 3. Force sensor mounted between robot's wrist flange and end-effector.

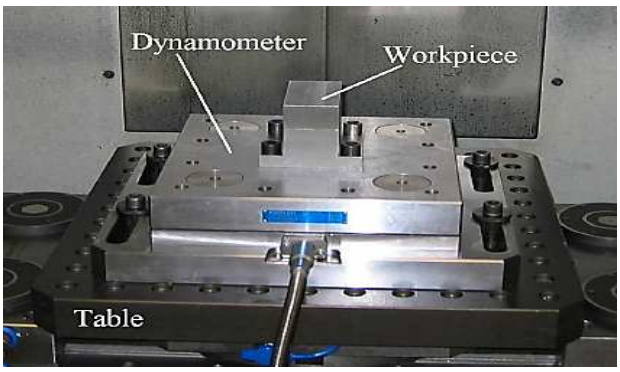

Fig. 4. Force sensor mounted between the workpiece and the workpost table.

Fig. 5. Kawasaki FS10E articulated-arm robot and Kawasaki D controller.

Table 1

Kawasaki FS10E robot parameters

Architecture	Articulated arm		
DOF	6		
Joint limits and speeds	Joint	Limits	Speed
	1	$\pm 160^o$	200 °/s
	2	$-105^o - 140^o$	140 °/s
	3	$-155^o - 120^o$	200 °/s
	4	$\pm 270^o$	360 °/s
	5	$\pm 145^o$	360 °/s
	6	$\pm 360^o$	600 °/s
Payload	10 kg		
Wrist load	Joint	Torque	Inertia
	4	21.5 N·m	0.63 kg·m^2
	5	21.5 N·m	0.63 kg·m^2
	6	9.8 N·m	0.15 kg·m^2
Repeatability	±0.1 mm		
Weight	170 kg		
Acoustic level	< 70 db		

Fig. 6. Robot tooling: ATI RC-340 end-effector.

Table 2

ATI RC-340 end-effector parameters

Motor type	air turbine
Idle speed	40000 rpm
Max. Torque	0.08 Nm
Power	340 W
Weight	1.2 kg
Compensation	max. ±7.5 mm, recommended ±3 mm
Compliance force	12.7–42 N at 1–4.1 bar
Spindle air speed	6.2–6.5 bar
Air consumption (idle)	2.8 l/s
Air consumption (stall)	10.2 l/s
Acoustic level	< 70 dB
Collet size	6 mm

a b

Fig. 7. The Kistler 9257B system: *a* – dynamometer; *b* – signal amplifier.

In order to provide support for the workpiece and the dynamometer, a T-slot plate was used. As shown in previous works, the accuracy of the robot varies inside its working space [3]. Thus, the position of the part was adjusted on the table so that it corresponded to the area in which the robot attains the best accuracy level.

To measure the machining forces appearing at the tool-part interface, a Kistler 9257B dynamometer was used (shown in Fig. 7) [11]. The dynamometer has high resolution, being able to measure machining force values in three orthogonal directions – corresponding to the three axes *X*, *Y* and *Z* of part's coordinates system. Also, the Kistler sensor does not affect the milling process, being stiff enough to measure force values up to 5 kN and measuring force values through four sensors and pressure-sensitive plates while maintaining the position of the workpiece. The data is collected through a signal amplifier (illustrated in Fig. 7) and sent to a computer using an acquisition board. Dedicated software displays the data in the form of a diagram and is able to export them in text format. The technical specifications of the Kistler 9257 B dynamometer are shown in Table 3 [11].

Taking into account that the milling tool is an important factor for the application, a suitable mill was chosen from ATI, dedicated for aluminium machining applications. The specifications for the milling tool are shown in Table 4 [10].

3. EXPERIMENTAL SETUP AND PROCEDURE

The T-slot plate was mounted on a metal frame fixed in front of the robot. The setup of the robotic cell for experimental determination is shown in Fig. 8.

Taking into account the technical specifications of the available equipment and the scope of the research, the part to be machined was chosen in the form of a 10 mm.

Table 3

Kistler 9257B parameters

Maximum values for measured forces	F_x, F_y, F_z	−5…5 kN
	F_z (for F_x and F_y ≤0.5F_z)	−5…10 kN
Overload	F_x, F_y, F_z	−7.5…7.5 kN
	F_z (for F_x and F_y ≤0.5F_z)	−7.5…15 kN
Threshold		< 0.01 N
Rigidity	C_x, C_y	> 1 kN/µm
	C_z	> 2 kN/µm
Natural frequency		3.5 kHz
Operating temperature		0…70 °C
Weight		7.3 kg
Clamping area		100 ×170 mm

Table 4

Milling tool parameters

	Model	ATI 9150-RC-B-24065
	Tool diameter	3/8"
	Length	5/8"
	Shank diameter	1/4"
	Materials	Aluminium, soft materials, plastics

Fig. 8. The setup of the robotic cell.

thick aluminium plate sized 200×300 mm. The operation performed was edge chamfering at 45°, as shown in Fig. 9. The milling operation was performed on three steps, each step with a radial depth of cut a_p of 0.1 mm. As the milling tool advanced from one step to another, due to the increasing width of the chamfer, the axial depth of cut increased too. Thus, the axial depth of cut a_e was 1.4 mm for the first step, 2.8 mm for the second step and 4.2 mm for the third step. Due to the increasing of the axial depth of cut, the chip width (and the load per tooth) also increased, leading to higher machining forces for each step, thus a higher load on the robot arm.

The programs were created using the block-teaching approach, so that each program line corresponded to one trajectory segment, as shown in Fig. 10. The block-teaching method has the advantage, for programs with simple structure, of easy modification for both position data and movement parameters. Also, the trajectory segments can be easily linked to corresponding program lines, making it easier to analyze robotic behaviour.

Fig. 9. The robotic chamfering operation; the gap used for evaluating the tool compliance behaviour can be seen on the edge of the part.

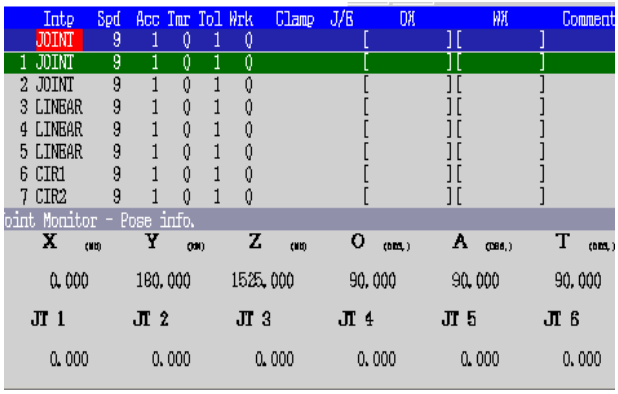

Fig. 10. Block teaching program structure.

In order to evaluate the behaviour of the radially compliant tool in milling operations and to observe the ability of the compliance system to follow the contour of the workpiece, a gap in the part edge was milled before the experimental procedure (as shown in Fig. 9). Afterwards, during experimental program runs, the machining tool, having the compliance pressure set to maximum value, executed the chamfering operation while running across the gap each time. The variations of machining forces were observed and analyzed around the gap and conclusions were drawn regarding the influence of the compliance system.

The experimental program was run a total of three times, each time the tool milling a depth of cut of 0.1 mm in the part edge. For each program run, the Kistler system recorded the force variations along the *X*, *Y* and *Z* axes as the tool moved on the path. Each resulting diagram (for each step, the *X* axis diagram, the *Y* axis diagram and the *Z* axis diagram – a total of 6 diagrams after all three experimental steps, shown in Figs. 11, 12 and 13) was exported into an Excel file. Furthermore, the dedicated software of the Kistler system combined the three measurements for each step - along the *X*, *Y* and *Z* axes – into a single diagram for easier comparative analysis.

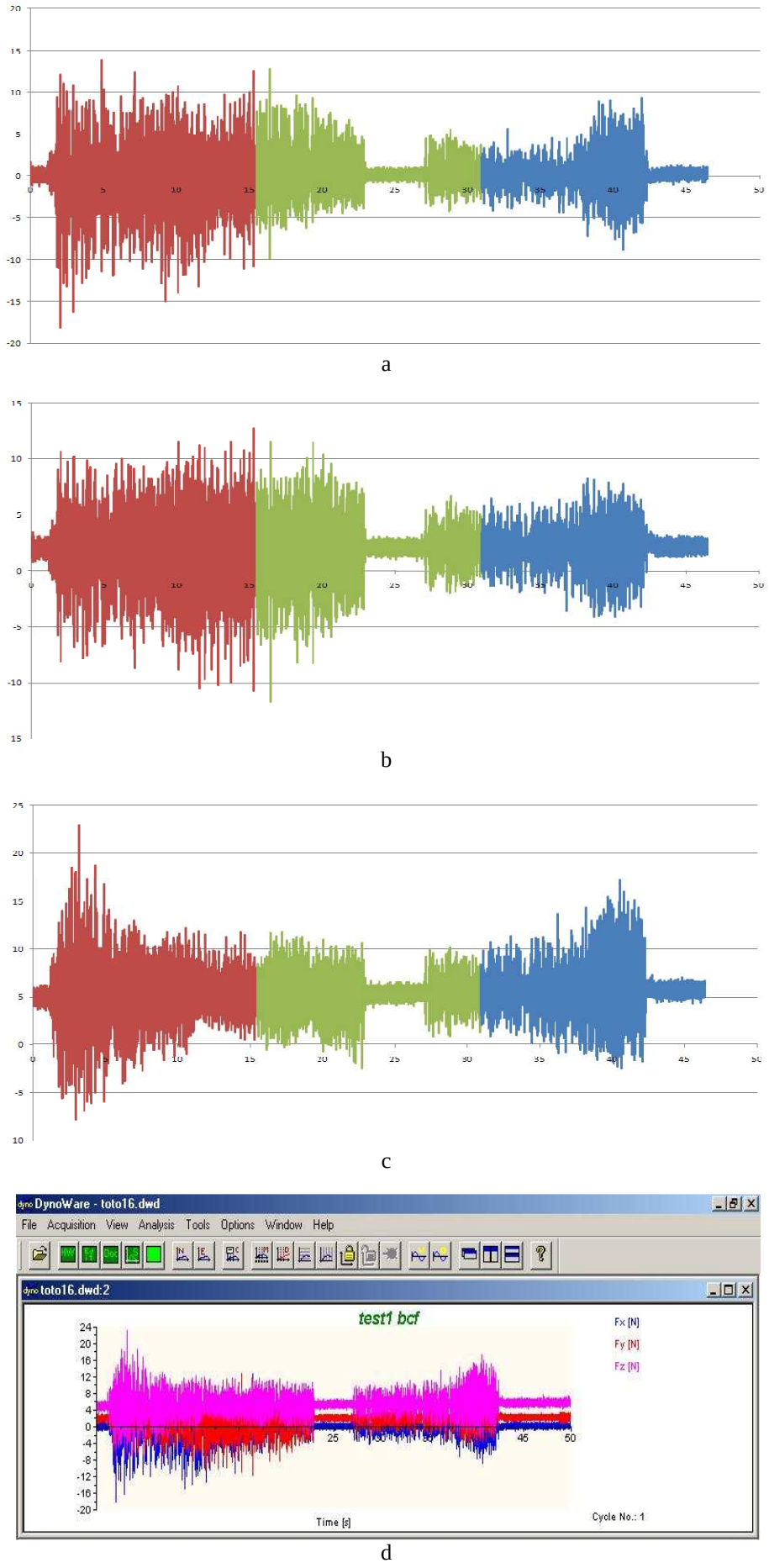

Fig. 11. The machining force for the first program run (a_e = 1.4 mm): *a* – machining forces along the *X* axis; *b* – machining forces along the *Y* axis; *a* – machining forces along the *Z* axis; *d* – machining forces measurements combined on the same diagram.

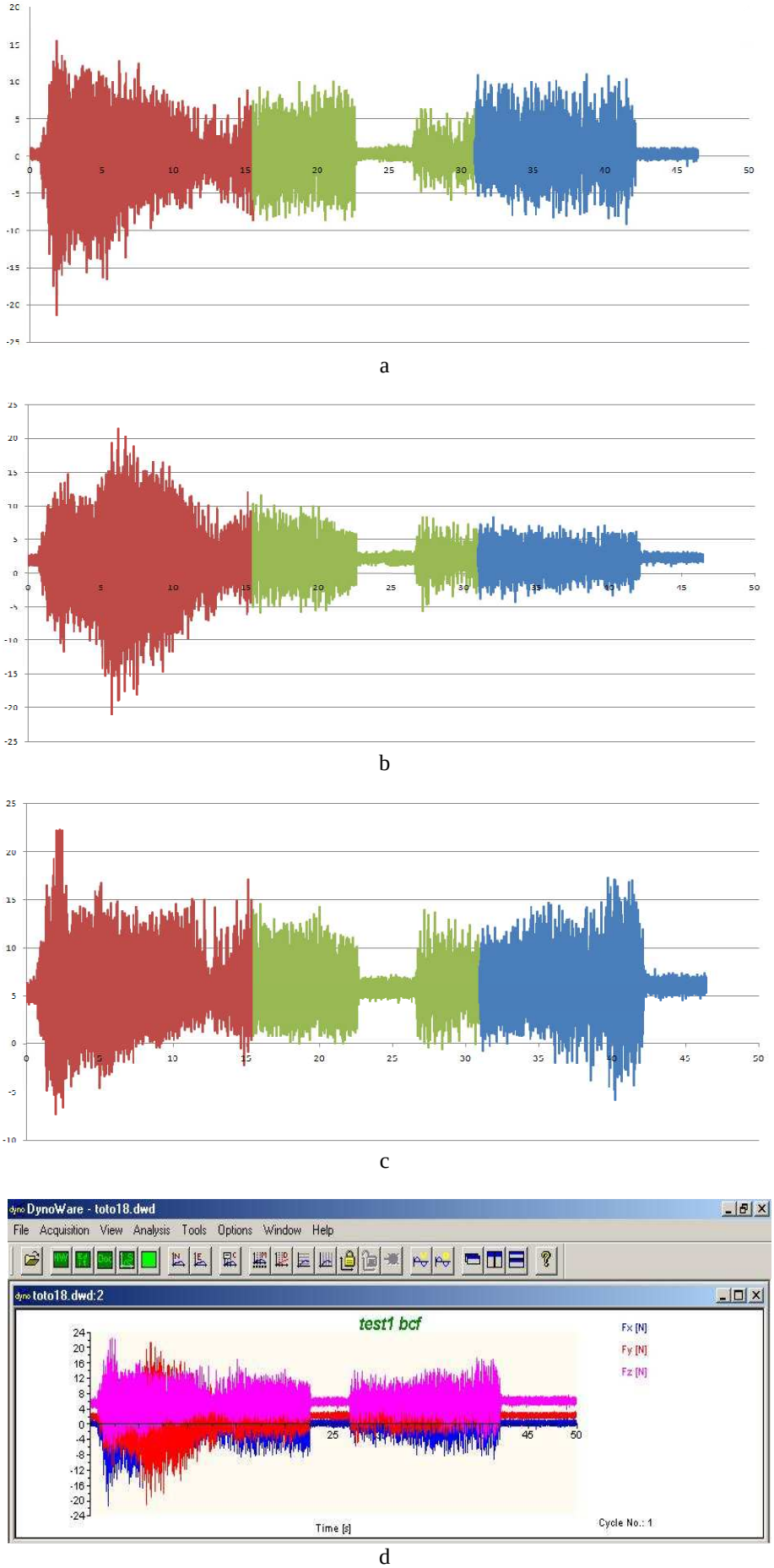

Fig. 12. The machining force for the second program run (a_e = 2.8 mm): a) machining forces along the *X* axis; – machining forces along the *Y* axis; *a* – machining forces along the *Z* axis; *d* – machining forces measurements combined on the same diagram.

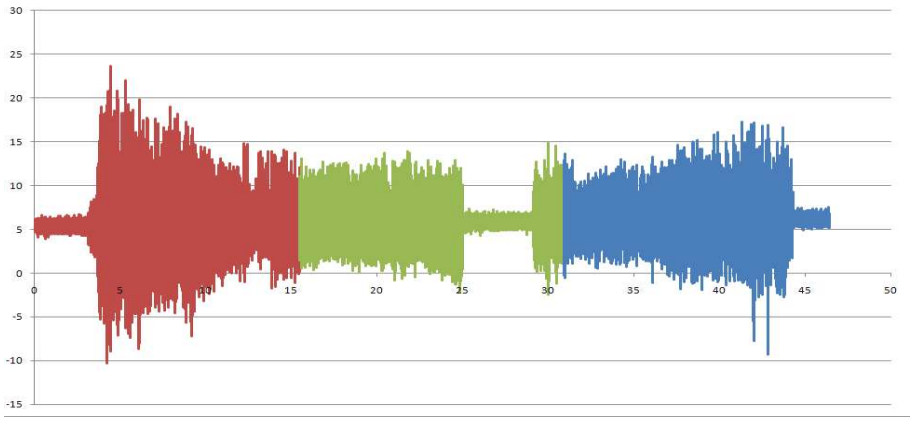

a

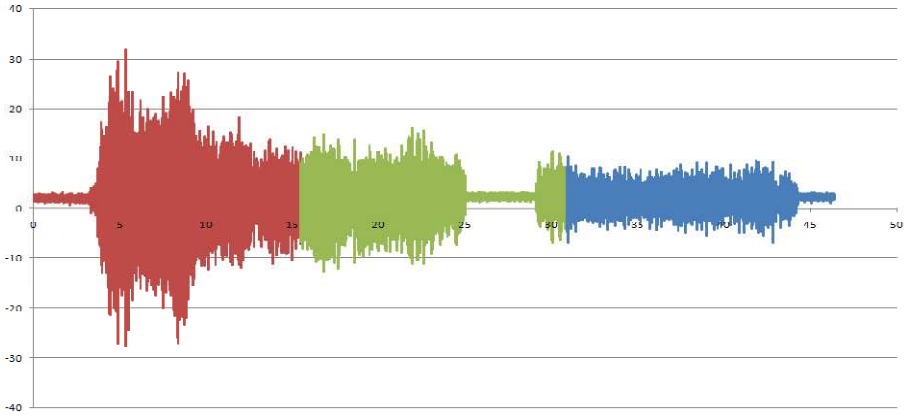

b

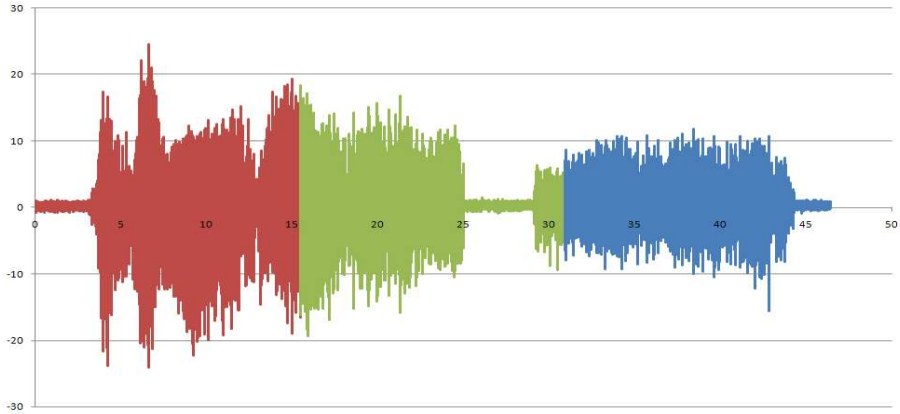

c

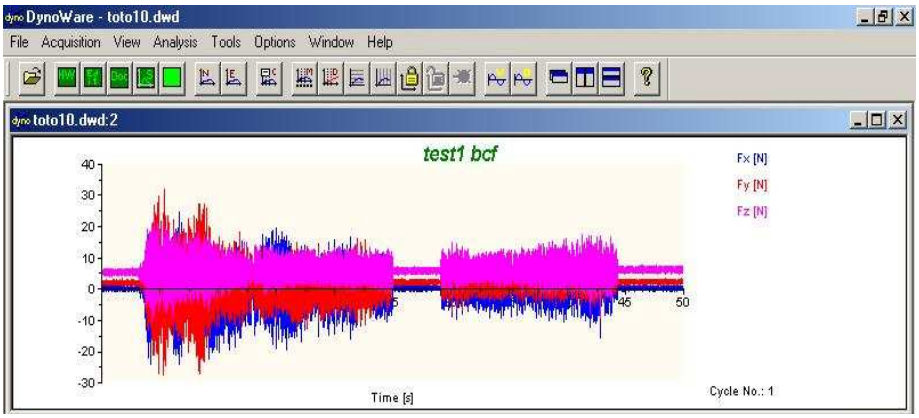

d

Fig. 13. The machining force for the third program run (a_e = 4.2 mm): *a* – machining forces along the *X* axis; *b* – machining forces along the *Y* axis; *a* – machining forces along the *Z* axis; *d* – machining forces measurements combined on the same diagram.

4. CONCLUSIONS

By analyzing the results obtained during the experimental procedures, a set of conclusions were drawn.

As it was expected, the machining forces had the lowest values during the first step of the experimental procedure (a_e = 1.4 mm). The maximum force values in this case were 15 N for the *X* axis measurement, 10 N for the *Y* axis measurement and 12 N for the *Z* axis measurement. Also, the median values of the machining forces were 5 N for the *X* axis measurement, 5 N for the *Y* axis measurement and 3 N for the *Z* axis measurement.

By analyzing the structures of the diagrams for the first experimental step, it was observed a significant level of chatter, especially in the *X* and *Y* directions. Because this chatter could not be caused by a lack of robot stiffness - as the robot payload is 10 kg., equivalent to a gravity force of 100 N, much higher than machining force values – it was concluded that the chatter was a result of the compliance system of the end-effector. Although the compliance pressure was set to maximum, the low value of the radial depth of cut resulted in a low thickness of the chip, so that the cutting was not done properly and the tool was deflected away from the part's edge.

Also during the first step, for the first part of the chamfering operation, when the tool engaged the part, the machining force was relatively high compared to the median value. The cause of this effect was the irregular cut partially caused by tool's compliance. The cut never stabilized along the path, but another increase in force peak values was observed at tool exit.

The machining forces had higher values during the second step of the experimental procedure (a_e = 2.8 mm). The maximum force values in this case were 15 N for the *X* axis measurement, 17 N for the *Y* axis measurement and 18 N for the *Z* axis measurement. Also, the median values of the machining forces were 5 N for the *X* axis measurement, 6 N for the *Y* axis measurement and 6 N for the *Z* axis measurement. Although the radial depth of cut was the same, the increase of the force values was caused by a higher axial depth of cut.

By analyzing the structures of the diagrams for the second experimental step, it was observed that the level of chatter is lower than in the first case. This was mainly a consequence of the increased thickness of the chips, which helped the tool keeping better contact with the edge of the part.

In the second stage of the experiment, when the tool engaged the part, the machining force was again relatively high compared to the median value, generating an irregular cut caused by tool's compliance. Nevertheless, in this case, the cut stabilized eventually after the first 20 mm of the path, resulting in a much better machining for the rest of the edge. It was also observed that, once stabilized, the cut was maintained within good parameters until the end of the operation.

The highest values of the machining forces were observed during the third and final step of the experimental procedure (a_e = 4.2 mm). This was an expected result, as the axial depth of cut and the chip thickness were higher than in previous cases. The maximum force values during this step were 22 N for the *X* axis measurement, 29 N for the *Y* axis measurement and 22 N for the *Z* axis measurement. Also, the average values of the machining forces were 10 N for the *X* axis measurement, 11 N for the *Y* axis measurement and 9 N for the *Z* axis measurement.

The structures of the diagrams for the third experimental step showed an acceptable level of chatter. Also, the chatter appeared mainly in the *Z* direction, while for the *X* and *Y* directions it was observed only at the beginning of the cut.

While the machining force at the beginning of the cut was again relatively high compared to the median value, the process stabilized much faster, and it was maintained within good parameters until the end of the operation.

Regarding the gap in the part's edge, by analyzing the configuration of force diagrams after passing the corresponding area, it was concluded that, in this case, the compliance of the tool helped in keeping a good contact with the part, as no disturbance in machining forces was observed after the tool re-engaged the workpiece. Thus, there is evidence that a radially compliant tool can help stabilizing the cut when irregularities are present in the part shape.

By taking into account the above facts, it can be concluded that, as long as the machining force is lower that the permissible load of the robot (the payload being, in this case, a good indicator), a heavier cut is desirable when machining with radially compliant tool in order to maintain good contact with the workpiece. Furthermore, it was observed that the compliance has both advantages and disadvantages: while it can cause a deflection of the tool away from the part's edge and chatter in some situations, it helps keeping good cutting condition if the part has irregularities.

REFERENCES

[1] J.J. Craig, *Introduction to Robotics: Mechanics and Control (Third Edition)*, Pearson Education, USA, 2005.
[2] A. Nicolescu, *Roboți Industriali*, Edit. Didactică și Pedagogică, 2005.
[3] A. Ivan, *Research regarding optimization of industrial robots for machining applications*, Doctoral Thesis, University "Politehnica" of Bucharest, 2011.
[4] http://www.robotics.org , accessed: 2015-11-24.
[5] http://new.abb.com , accessed: 2014-03-16.
[6] B. Siciliano, O. Khatib, *Handbook of Robotics*, Springer, Stanford, 2008.
[7] http://www.expo21xx.com/sensor , accessed: 2016-07-08.
[8] http://www.researchgate.net, accessed: 2016-04-03.
[9] https://robotics.kawasaki.com, accessed: 2016-02-23.
[10] http://www.ati-ia.com/, accessed: 2016-03-15.
[11] http://www.kistler.com , accessed: 2011-08-12.